Sensors & Transducers, Vol. 223, Issue 7, July 2018, pp. 9-21

www.sensorsportal.com

Sensors & Transducers

Published by IFSA Publishing, S. L., 2018
http://www.sensorsportal.com

Properties of Hydrogen Peroxide Sensors Made from Nanocrystalline Materials

Vladimir M. Aroutiounian
Yerevan State University, Yerevan 0025 Alex Manoukian Str. 1, Armenia
Tel.: 37460710311, fax: 37460710355
E-mail: aroutiounv1@yahoo.com

Received: 26 March 2018 /Accepted: 5 July 2018 /Published: 31 July 2018

Abstract: The determination of trace amounts of hydrogen peroxide is important in medical, environmental, pharmaceutical, and biological fields as well as in food and textile industry due to a wide spectrum of antibacterial properties, low toxicity and ecological purity. It is necessary to determine the concentration of hydrogen peroxide (H_2O_2). Several techniques have been developed for a reliable and sensitive determination of H_2O_2 such as chemiluminescence, spectrophotometry, fluorimetric and colorimetric detection, liquid chromatography, optical interferometry. These techniques are complex, expensive and time consuming.
Earlier hydrogen peroxide sensors made from organic materials. Now electrochemical sensors are mainly used. In recent years, nanotechnology progress is promoted advance in the field of manufacturing of the H_2O_2 sensors. New sensors for H_2O_2 vapor have been developed using a semiconductor. Metaloxides, carbon nanotubes and graphene can be used. Nanostructured sensors for detection of hydrogen peroxide vapors were developed recently. All these versions of sensors and their main characteristics are reported in this review.

Keywords: Hydrogen peroxide, Sensor, Metaloxides, Carbon nanotubes, Graphene.

1. Introduction

The determination of trace amounts of hydrogen peroxide is important in medical, environmental, pharmaceutical, and biological fields as well as in food and textile industry due to a wide spectrum of antibacterial properties, low toxicity and ecological purity. It is necessary to determine the concentration of hydrogen peroxide (H_2O_2), not only in chemical and industrial processes (for example, disinfection, waste-water treatment), but also as an intermediate product of an enzyme reaction in biochemical processes (for example, glucose determination). Therefore, a hydrogen peroxide sensor can be also used as an intermediate transducer for other biosensors.

However, pure H_2O_2 at large concentrations is explosive under certain conditions (for example, in the presence of transition metals). Therefore, concentrated solutions of H_2O_2 can cause burns in the case of the contact with skin, mucous membranes and respiratory tract. H_2O_2 is subsumed under the category of matters those are dangerous for man with certain maximum permissible concentration. Therefore, the development of sensors for determination of the H_2O_2 concentration in the environment is important and attracts interest of chemists, physicians, industrial engineers, etc. The H_2O_2 stable sensors can be used in in various fields of the industry and analytical chemistry, for the environmental control, in clinical diagnostic. In biology and physiology, H_2O_2 has been recognized as a gesturing molecule for precise and prompt determination of oxidative stress that can be associated with different kinds of chronic diseases such as Alzheimer's, atherosclerosis, lungs injury,

cardiovascular diseases, parasitic infections, diabetes, cancer and so on. It is not only a byproduct of numerous oxidases in various biological functions, but also a requisite mediator in biomedical, pharmaceutical, food and environmental analysis. In living systems, its massive accumulation is detrimental for normal growth of cells and is engendered by the oxidative mitochondrial functions, incomplete reduction of oxygen and metabolic reactions occurring in live cells [1-2]. It is noteworthy that H_2O_2 and other reactive oxygen species play a critical role in proliferation, physiological intracellular signaling transduction, straddling development, abiotic anxiety influences, response to lethal attacks, relocation and distinction of healthy cell [3]. Nevertheless, the excessive production of H_2O_2 in cellular environments causes its penetration to other cellular compartments and is extremely pathogenic to living organisms [4-5]. Therefore, the determination of exact level of H_2O_2 paves the way for understanding the pathological, physiological and biomedical role of H_2O_2 [6].

Several techniques have been developed for a reliable and sensitive determination of H_2O_2 such as chemiluminescence, spectrophotometry, fluorimetric and colorimetric detection, liquid chromatography, electroanalytical and optical interferometry [7-12]. These techniques are complex, expensive and time consuming. Now electrochemical sensors are mainly used [11-15]. A large range of materials such as ferric hexacyanoferrate (Prussian blue) and other metal hexacyanoferrates, metallophthalocyanines and metalloporphyrins, transition metals and metal oxides have been employed for the manufacture of these sensors. The advantages of these sensors are simplicity of manufacturing, good response and capability of control in a real time. In recent years, nanotechnology progress is promoted advance in the field of manufacturing of the H_2O_2 electrochemical sensors. For example, carbon nanotubes and graphene can be used either as substrates with high specific area for catalytic materials or as electrocatalysts by themselves [16-18].

H_2O_2 serves as a disinfectant for medical equipment and surfaces as well as for sterilizing surgical instruments. Therefore, the correct selection of the H_2O_2 concentration during the sterilization of the equipment technological surfaces and also control of the H_2O_2 content in air after completion of disinfection cycle are very important. Note that the process of chemical decontamination can be carried out in two different ways: the first one is the wet approach using water or any other solutions of H_2O_2 (certain concentration) and the second one is the dry method using H_2O_2 in vapor phase [19]. Therefore, the development and manufacturing of stable and reproducible sensors sensitive to H_2O_2 vapors are extremely required [20-22]. The checking of H_2O_2 vapors phase is also crucially significant in connection with counterterrorism efforts. The sensors sensitive to H_2O_2 vapors may find application in the detection of peroxide-based explosives. The most used method is based on the determination of the concentration of H_2O_2 vapors after cooling down and being absorbed in the water. The near infrared spectrophotometry was used for the monitoring of the concentration of H_2O_2 vapors in the course of sterilization [20].

The chemiresistive films made from organic p-type semiconducting phthalocyanines metalized with elements of p-, d-, and f-blocks were sensitive to H_2O_2 vapors [18]. An amperometric sensor for detection of H_2O_2 vapors made of an agarose-coated Prussian-blue modified thick-film screen-printed carbon-electrode transducer was investigated [21]. It was reported about organic single-wire optical sensor for H_2O_2 vapours made of organic core/sheath nanowires with wave guiding core and chemi-luminogenic cladding [22].

A new type of concentration sensor for H_2O_2 vapor has been developed in [21] by making use of a semiconductor. Output from the vapor sensor has been shown to have a good linear relationship with the logarithm of the concentration of H_2O_2 vapor. Concentration of H_2O_2 vapor introduced into the sterilization chamber was kept constant. The hydrogen peroxide sensor has been calibrated and standardized by using the standard H_2O_2 vapor whose concentration has been determined by calculating partial pressure of H_2O_2 over the water- H_2O_2 solution. It indicated that the sterilization by H_2O_2 vapor can be validated as precisely as steam sterilization by measuring and controlling the concentration of hydrogen H_2O_2 peroxide vapor using a combination of the H_2O_2 concentration sensor and the vapor generator. Influence of temperature and humidity have also been studied.

Hydrogen peroxide bio-decontamination Bioquell equipment is proposed [www.bioquell.com].

2. Hydrogen Peroxide Sensors Using Organic Materials

Possibilities of monitoring of vapour phase hydrogen peroxide (VPHP) decontamination process were investigated by group headed by P. Kačer [20, 28]. Polymer matrix based methylene blue sensors based on its spectra changing in VPHP were developed.

A novel nonenzymatic H_2O_2 sensor has been fabricated and investigated in paper [29]. By dispersing copper nanoparticles onto polypyrrole (PPy) nanowires by cyclic voltammetry (CV) to form PPy-copper nanocomposites on gold electrodes. It was proved [29] that the PPy-copper nanocomposite showed excellent catalytic activity for the reduction of H_2O_2. The sensor showed a linear response to hydrogen peroxide in the concentration range between 7.0×10^{-6} and 4.3×10^{-3} mol L^{-1} with a high sensitivity, and a detection limit of 2.3×10^{-6} mol L^{-1}. Experiment results also showed that the sensor had good stability.

The possibility for improving of analytical performances for nanostructuring of Prussian blue

(PB) have been reported in [12]. It is possible by electrodeposition of nanostructured PB films. Analytical performances of the resulting PB based nanoelectrode arrays have been studied in course of H_2O_2 detection. The value of sensitivity for sensors was 0.2 A M^{-1} cm^{-2}, which is more than for electrodes modified by PB electrodeposited through liquid crystal template. Detection limit was 10^{-8} M and a linear calibration range was extending over six orders of magnitude of H_2O_2 concentrations, which are the most advantageous analytical performances in hydrogen peroxide electroanalysis. The possibility for improving of analytical performances for nanostructuring of Prussian blue (PB) have been reported in [12]. It is possible by electrodeposition of nanostructured PB films, which are H_2O_2 acts as a powerful oxidizing agent, so it could be applied in many organic compound synthesis reactions [31].

3. Hydrogen Peroxide Sensors Made from Metaloxides

A glassy carbon and indium tin oxide (ITO) electrodes have been modified in [32] with the nano TiO_2–Au–KI film by the adsorption of TiO_2 nanoparticles on the electrodes followed with the electrochemical depositions of nano Au and KI film. Further the nano TiO_2–Au–KI film modified ITO was examined. From the microscopic results, the adsorbed nano TiO_2 particles size were found in the range of 70–100 nm. Here the electrochemical depositions of nano Au were formed as a flower shape were in the size range of 230 nm to 1 mcm. The electrochemical behavior of nano TiO_2–Au–KI film has been examined in different pH solutions. The linear range of detection for H_2O_2 oxidation using nano TiO_2–Au–KI film was found as 1×10^{-5} to 1×10^{-4} M and 1×10^{-9} to 1×10^{-7} M in CV and differential pulse voltammetry (DPV) techniques. Differential pulse voltammograms of nano TiO_2–Au–KI film are shown in Fig. 1. It shows the DPVs of nano TiO_2–Au–KI film (pH 7 PBS) for the different concentrations of H_2O_2. Here the DPVs were recorded by sweeping the potentials in the range of 0–0.9 V at pulse amplitude of 50 mV, and a scan rate at 50 mVs^{-1}. Here the DPVs were recorded in the concentration range of 1×10^{-9} to 1×10^{-7} M H_2O_2, respectively. Curve a–g in Fig. 1 shows the well-defined and stable anodic peak current curves for H_2O_2 oxidation. These anodic DPV curves confirm the H_2O_2 oxidation process on the TiO_2–Au–KI film modified GCE. Further the oxidation peak currents of H_2O_2 increases linearly with the increasing concentration of H_2O_2, respectively.

The inset of Fig. 1 shows the current vs. concentration plot for the electrocatalytic oxidation of H_2O_2.

From the above results, it shows that the nano TiO_2–Au–KI film modified GCE is effective for the electrocatalytic oxidation of H_2O_2 in nanomolar concentration range by using DPV techniques.

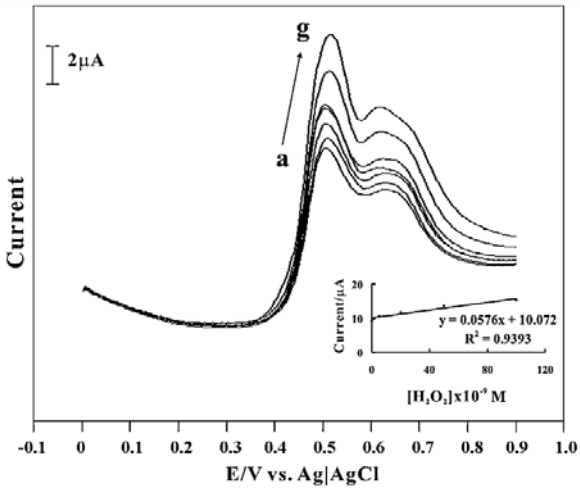

Fig. 1. Differential pulse voltammograms of nano TiO_2 – Au–KI film modified GCE in pH = 7 (containing 1×10^{-3} M KI) with various concentration of H_2O_2 (a–g) 0, 1×10^{-9}, 5×10^{-9}, 1×10^{-8}, 2×10^{-8}, 5×10^{-8} and 1×10^{-7} M.

The practical applications of nano TiO_2–Au–KI film was evaluated by analyzing the real samples such as antiseptic and contact lens cleaner solutions containing H_2O_2.

Structurally integrated metal oxide intercalated layered double hydroxide (LDH) nanospheres (NSs) hybrid material has been of considerable current interest [33]. A new type of MnAl LDH wrapped CuO (CuO@MnAl LDHs) NSs by anchoring CuO nanoparticles (NPs) with MnAl LDHs via a facile co-precipitation and hydrothermal approach was reported. Its practical application as high-efficient electrocatalyst towards H_2O_2 reduction for biological application was explored. The integration of n-type spinel of CuO and p-type semiconductive channels of MnAl LDHs can accelerate electron transfer at breakdown voltage of p-n junction. Owing to the synergistic effect of the high surface area of CuO NPs, superb intercalation features of semiconductive MnAl LDHs for encapsulating NSs, and their intrinsic p-n junction characteristics, CuO@MnAl NSs have exhibited excellent electro-catalytic activity towards the reduction of H_2O_2. When implemented in electrochemical sensor system, the CuO@MnAl NSs modified electrode displays high nonenzymatic sensing performances towards H_2O_2, detection limit, good selectivity and long term stability.

Hollow-sphere Co_3O_4 nanoparticles were successfully synthesized [34-41]. It is found that the as-prepared Co_3O_4 nanoparticles possesses uniform hollow spherical structure with many voids on the surface. It's worth noting that the high density of metal sites, the ordered arrangement of Co, as well as the uniform crystal size and regular morphology resulting in an excellent accessibility of Co. The resulting Co_3O_4 hollow sphere was exploited as an electrocatalyst for sensitive H_2O_2 detection in an alkaline medium. The Co_3O_4 hollow sphere modified glassy carbon electrode exhibited a fast response time (within 3s), a high sensitivity of 120.55 μA/mM

(959.79 mkA.mM^{-1}cm^{-1}), a broad linear range from 0.4 mM to 2.2 mM, a detection limit of 0.105 mM (S/N=3), and good stability and selectivity, suggesting its excellent performance towards H_2O_2 detection [34].

A rapid, reproducible, cost-effective approaches for the detection of H_2O_2 has been developed in [42] based on the change of localized surface plasmon resonance (LSPR) peak of Au nanorods (NRs). A method for detecting the concentration of H_2O_2 based on the change of LSPR of Au NRs was developed. H_2O_2 can etch Au NRs due to higher standard redox potential. The absorption spectra showed that various ratio of LSPR peaks is proportional to the concentration of H_2O_2, which suggested that Au NRs can potentially serve as a new sensor for the detection of H_2O_2.

4. Hydrogen Peroxide Sensors Made from Metaloxides and Graphene

A new electrocatalyst, MnO_2/graphene oxide hybrid nanostructure was synthesized for the detection of H_2O_2 [43]. The MnO_2/graphene oxide based electrodes showed high electrochemical activity for the detection of H_2O_2 in alkaline medium. Manganese dioxide (MnO_2) is a kind of attractive inorganic material and can catalyze the electrocatalytic ability towards H_2O_2. [19-20]. The GO/MnO_2 electrode presents high sensitivity, low potential and long-term stability towards the detection of H_2O_2. Amperometric response of the graphene oxide/MnO_2 electrode to H_2O_2 is shown in Fig. 2.

The preparation of NiO/graphene (NiO/GR) nanocomposite for determination of H_2O_2 was reported in [44]. The electrocatalytic behaviors towards H_2O_2 are investigated by cyclic voltammetry and chrono amperometry in alkaline aqueous solution.

High electrocatalytic activity toward the oxidation of H_2O_2 was observed with detection limit of 0.7664 μM, high sensitivity of 5 91 μAmM^{-1} cm^{-2}, a wide linear range of 0.25–4.75 mM.

A novel nonenzymatic, amperometric sensor for H_2O_2 was developed in [45] based on an electrochemically prepared reduced graphene oxide (RGO)/zinc oxide (ZnO) composite. RGO/ZnO composite was fabricated on a glassy carbon electrode (GCE) by a green route based on simultaneous electrodeposition of ZnO and electrochemical reduction of graphene oxide (GO).

The electrochemical performance of the RGO/ZnO composite modified GCE was studied by amperometric technique, and the resulting electrode displays excellent performance towards H_2O_2. At −0.38 V in the linear response range from 0.02 to 22.48 mM, with a correlation coefficient of 0.9951 and short response time (<5 s). The proposed sensor also has good operational and storage stability with appreciable anti-interfering ability.

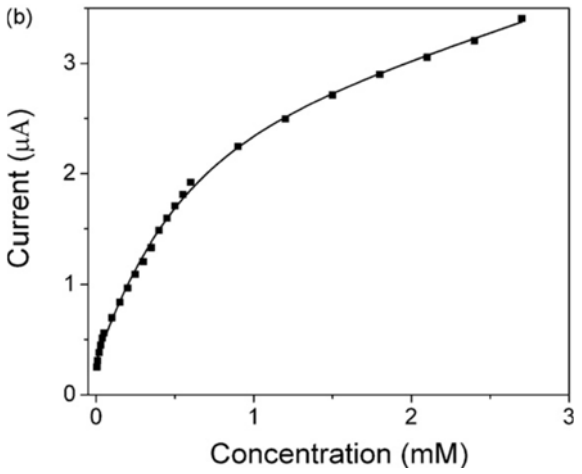

Fig. 2. Amperometric response of the graphene oxide/MnO_2 electrode upon addition of H_2O_2 at −0.3 V. (b) The corresponding calibration curve between the current response and concentration of H_2O_2.

Note that graphene and graphene oxide are very promising materials for manufacturing of other chemical sensors (see, for example, papers [46-53]).

Let continue short description of H_2O_2 sensors using graphene and graphene oxide. The catalytic activity of N-doped graphene toward a peroxidase substrate oxidation in the presence of H_2O_2 is presented in [53]. In addition, the activity was compared with that of metallic nanoparticles decorated graphene, achieved either by catalytic chemical vapor deposition with induction heating or by chemical reduction of graphene oxide (GO). From all investigated graphene-based nanomaterials, the highest activity was exhibited by N-doped graphene and gold nanoparticles supported on chemically reduced graphene oxide. The steady-state kinetic of the two nanocomposites was carried out in order to evaluate their peroxidase-mimetic activity. Doping the graphene surface with nitrogen atoms led to a nanomaterial with a better affinity toward H_2O_2 compared to the natural enzyme (horseradish peroxidase). Additionally, the systematic study of the catalytic activity for a variety of graphene-based nanomaterials offered important findings for designing new nanomaterials with peroxidase-like activity. The sensing applications presented here are offering a useful comparison of the peroxidase like ability of a large variety of graphene-based nanomaterials. The results are showing that the oxidation of benzidine derivatives in the presence of H_2O_2 by graphene nanocomposites is mainly due to the known catalytic activity of the superficial metallic nanoparticles and/or the residual functional groups existing in the chemically obtained graphene based composites. Moreover, in comparison with natural enzymes, doping the graphene surface with nitrogen atoms (N-Gr) led to the formation of a promising platform for building new enzyme mimic nanomaterials.

Graphene oxide nanoribbons (GONRs) were synthesized in the work [54] via the longitudinal unzipping of multi-walled carbon nanotubes (MWCNTs) nanoparticles with the aid of strong oxidants. TheMnO_2/reduced graphene oxide nanoribbons (MnO_2/rGONRs) composites were fabricated by means of a reproducible and single-step hydrothermal co-reduction of $KMnO_4$ and GONRs. MnO_2/rGONRs exhibited high electrochemical response toward H_2O_2.

The developed nonenzymatic electrochemical sensor exhibited well-defined amperometric response towards H_2O_2 in a wide linear range of 0.25–2245 M (see Fig. 3), and a detection limit of 0.071 M (S/N = 3) could be obtained. The proposed sensor displayed excellent electro-chemical analytical performance, acceptable reproducibility, high accuracy, and great anti-interference ability.

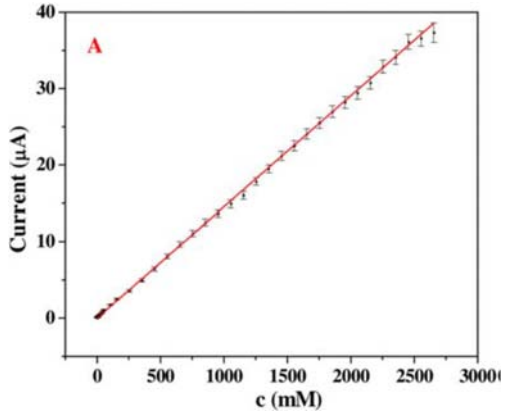

Fig. 3. The corresponding calibration curve of the MnO_2/GNRs/GCE in the H_2O_2 concentration range of 0.25–2455 M.

Au nanoparticles and reduced graphene oxide (r-GO) co-modified TiO_2 nanotube arrays (TNTs) were prepared in [55] by a facile and green strategy based on the electro-deposition technology for detecting H_2O_2, O_2 and nitrite. A highly ordered TiO_2 nanotubes was synthesized based on anodic oxidation method, and Au nanoparticle sand reduced graphene oxide were electro-deposited on the membrane to fabricate an electrochemical electrode. The established Au/r-GO/TNTs electrode is as a novel electrode system for H_2O_2 detection with a quick response H_2O_2 at −0.3 V with a high sensitivity (1011.35 mA $M^{-1}cm^{-2}$), wide linear range (0.01–22.3 mM), low detection limit (0.006 mM), good stability and enzyme-like selectivity. In addition, it holds great promise to the preparation of electrochemical sensing and biosensing platform based on the electrocatalytic behaviors of different kinds of important electroactive compounds such as dissolved O_2 and nitrite ion. As is demonstrated in [55], r-GO sheets are uniquely advantageous to serve as a conductive support to uniformly anchor Au nanoparticles with well-defined size and shapes, in which the agglomeration of Au nanoparticles in common electrode is avoided. Based on the particular architecture and novel performance, the Au/r- GO/TNTs hybrid could be an extremely promising candidate applicable for a wide range of electrochemical sensing and biosensing applications.

Series of $FeVO_4$ materials with different morphologies were prepared in [56] through a facile hydrothermal method and were studied as peroxidase mimics. The different pH values during the preparation process led to different crystal structures, morphologies and peroxidase-like activities of the as-prepared $FeVO_4$ products. $FeVO_4$-4 NBs exhibited the best intrinsic peroxidase-like activity compared to other $FeVO_4$ materials owing to its nanobelt structure combined with a large BET specific surface area. On account of its excellent peroxidase mimic activity of $FeVO_4$-4 NBs, a novel ultrasensitive system for optical detection of H_2O_2 was established, and the detection limit of H_2O_2 could reach 0.2 mM. Besides, $FeVO_4$-4 NBs exhibited good selectivity, reproducibility, long-term stability, and easy recovery property benefited from its chemical stability and magnetic property. This work provides a novel, fast response, low cost, accessible and highly sensitive system for visual detection of H_2O_2.

A novel TiO_2-encapsulated Au (Au@TiO_2) yolk-shell nanostructure was synthesized in [57] via a method, in which the TiO_2 nanotubes could effectively restrain the aggregation and growth of Au nanoparticles and supply more active sites and high surface areas for biocatalytic reactions. On the basis of the highly efficient peroxidase-like activity of Au@TiO_2, an effective method for colorimetric detection of H_2O_2 and glucose was established. Considering numerous advantages including reduced aggregation, good chemical stability and high catalytic activity available by the present Au@TiO_2 with unique structure, designing other yolk-shell nanostructures with exact function orientation using a similar strategy may also be very promising in the application of biocatalysis and bioassays.

A novel strategy to synthesize elegant Au@ TiO_2 yolk-shell nanostructures used as peroxidase-like enzymes was developed. Their applications for colorimetric detection of H_2O_2 and glucose were investigated. Benefited from the effective combination of high controllable technology involved in ion sputtering and atomic layer deposition, the prepared Au@TiO_2 nanocomposites had uniform morphology with well-dispersed Au nanoparticles confined in TiO_2 nanotubes. The Au@TiO_2 exhibited remarkably decent intrinsic peroxidase-mimic activities and was highly dependent on the pH, temperature and the concentration of reactants.

Nanozymes, as the next-generation artificial enzymes, have attracted wide interest in recent years [58]. Compared with natural enzymes, nanozymes, with their advantages of high stability against denaturing, low-cost, easy storage and treatment are attractive and promising candidates in chemical sensing, immunoassay development, cancer diagnostics and therapy, and environmental protection [59]. At present, a large number of nanoparticle (NP)

artificial enzymes have been constructed to mimic natural enzymes, including iron oxide-based NPs with peroxidase and catalase-like activities [60-61], cerium oxide-based nanomaterials with oxidase, catalase and SOD mimetic properties [62-63], cobalt oxide ones that are peroxide and catalase mimics [64-65], copper oxide and manganese dioxide nanomaterials that display oxidase-like activity [66-67], vanadium pentoxide peroxidase mimics [68], and metal/bimetal-based [69] and carbon-based NPs [70] with oxidase, peroxidase, and SOD mimetic activity.

A new V_2O_5 nanozymes-based colorimetric assay has been developed for H_2O_2 and glucose detection. Under the optimal reaction conditions, the method showed good responses toward H_2O_2 with a linear range from 1 to 500 M. The result shows that the proposed assay method for H_2O_2 and glucose based on V_2O_5 nanozymes has a wide linear range, and is simple, fast, and sensitive.

5. Hydrogen Peroxide Sensors Made from Carbon Nanotubes

Our investigations of gas sensors made from different metal oxide composites with carbon nanotubes (CNTs) [71-77] shown the following:

1. Use of pristine CNT as sensors does not promising.

2. Functionalization of CNTs can be made with organic materials. Hyper sensibility and selectivity of detection of CO_2, NH_3, O_2, Cl_2, HCl, dimetyldimetylphosphate observed by CNT nanocomposites, covered with polyethylene, polyanylyne and polypyrrol.

3. CNTs, decorated with Pd, Rh, Au and Ni nanoparticles are suggested for detection of H_2S, CH_4, H_2, CO, O_3, C_6H_6, NH_3, NO_2, and C_2H_5OH up to their ppb level.

4. Special interest is attended to investigation of possibilities of manufacture of CNT functionalized (decorated) with different metal oxide composites. Most of its are carried out by CNT, decorated with SnO_2. Modifications of such nanosensors surface with precious metals led to remarkable improve of the sensitivity and selectivity of sensors.

5. Sensibilisation of CNT- SnO_2 composites in water solutions of Ru (OH) Cl_3 leads to high response to hydrogen as well as to synergistic effect during detection of isobutene and the lowering of temperature of pre-heating of work body of sensors up to 150-200 °C. Such sensors are sensitive also to vapors of VOC gases (acetone, toluene, ethanol and methanol) at approving the same temperatures of pre-heating.

6. Thin film (including 1D film) nanosensors of ethanol vapors were manufactured on the base of CNT-Fe_2O_3 solid solutions. Sensors of H_2, NO_x and CO were manufactured from CNTs with cobalt oxide, $Co_{1-x}N_xFe_2O_4$, CuO and WO_3.

7. Substantial interest invokes research and development of nanosensors working without pre-heating of their work body (at room temperature). 10 %- SnO_2 – CNT nanocomposite sensor detected ammonia and NO_2. Doping of CNT with N and B and its synthesis with metal oxide SnO_2 allowed dramatically increase the conductivity of the nanosensor and response to CO and NO_2. Nanosensors made from Co_3O_4- SnO_2 and Pt/TiO_2/CNT were sensitive to H_2, NH3 and O_3 on the 20 ppb level of gas concentration.

8. Nanosensors made from all mentioned composites CNT-metal oxides had lowest response and shorter times.

9. It is clear that the doping of metal oxides with CNTs lead to greater sensitivity to gases, better speed to response of nanosensors and a lowering of temperature of pre-heating of their work body (up to room temperature, when the pre-heating is not necessary). Possible mechanisms of the response of developed sensors to gases are discussed. Doubtless, that different type of conductivity of CNTs and metaloxides, change in the work function (high of potential barrier), modulation of formed heterojunctions should be take into account at the analysis of complicate processes and phenomena in gas sensitive structures reported above.

Nanostructured Sensors for Detection of Hydrogen Peroxide Vapors (VPHP) were presented in [78]. The sensor chip with sensors on it was sat in the ambient air. When the output of H_2O_2 mixture blow to the sensors, the change of resistances was multiplexed and recorded. The recorded response curve shows 1) the base resistance of sensors during the pure carrier gas exposure and then 2) the change of the resistance due to the sensor response to the H_2O_2 while the syringe pump injected the saturated H_2O_2 of 50 % H_2O_2 in water with different pump rates for different concentrations. The sensor response is from pristine carbon nanotubes interact with the H_2O_2 molecules. There are 3 replicates of the H_2O_2 exposures at each concentration. The repeatability is varied from 0.21 % to 0.47 % for different concentrations in terms of standard deviation calculated from 3 repeat responses. The response time included the sample injection time is in seconds to the full responses for all the exposures and the recovery time are also in seconds. This fast response enables reported sensors for high through put airport security inspection. The quick response to the H_2O_2 injection and reach to the full response enables the accurate measurement for low false alarm rate.

The responses to H_2O_2 may be due to the partially (weak) oxidation of carbon nanotubes by H_2O_2 molecules. The calibration curve of the sensor response vs. the concentration of H_2O_2 shows that the response is proportional to the logarithmic concentration of H_2O_2. This relationship reveals that there H_2O_2 is a charge transfer interaction between the carbon nano-tubes and the H_2O_2 molecules. The pristine carbon nanotubes as a sensing material for H_2O_2 detection have selected. From sensor testing results, it shows the sensor response time was in seconds, gives clear sensing signal to 50 ppm H_2O_2 in air at room temperature, recovered very fast for reuse

in the field. With a reduction of the noise, our sensor should be able to detect 1ppm and lower.

Silver particles were patterned on flexible and transparent single-walled carbon nanotube (SWCNT) films using the electrochemical deposition method, and these patterned silver particles were then used as electrodes to detect H_2O_2 [79]. The sizes and densities of silver particles were tuned by varying the patterned design and the preparation conditions. Field emission-scanning electron microscopy revealed that the patterned silver particles were homogeneously distributed on the SWCNT films (AgPs-SWCNT), with an average size of 150–200 nm.

The AgPs-SWCNT sensor had excellent electro-catalytic activity for detection due to the unique electrocatalytic properties of the silver particles and the good conductivity of the SWCNT film. The amperometric response of the electrode was rapid (within 2 s), sensitive to a wide linear range of H_2O_2 from 0.016 mM to 18.085 mM, had high sensitivity and a low detection limit (2.76 M) for H_2O_2. Moreover, the AgPs-SWCNT film sensor was selective for H_2O_2 and was stable over a long period of time.

Nanostructured Sensors for Detection of Hydrogen Peroxide Vapors Solid-state VPHP sensors made from doped metal oxide ZnO<La> and SnO2<Co> were prepared in [80] for detection of H_2O_2 vapors. Ceramic targets made from metal oxide ZnO doped with 1 at.% La or SnO_2 doped with 2 at.% Co were synthesized by the method of solid-phase reaction in the air. The following program of annealing for the compact samples of ZnO<La> was chosen: rise of temperature from room temperature up to 1300 °C for three hours, soaking at this temperature during four hours, further decrease in the temperature for three hours prior to room temperature. The annealing of the compacted samples SnO_2<Co> was carried out at 500 °C, 700 °C, 1000 °C and 1100 °C consecutively, soaking at each temperature during five hours. Then, the synthesized compositions were subjected to mechanical treatment in the air in order to eliminate surface defects. Thus, smooth, parallel targets with a diameter ~ 40 mm and thickness ~2 mm were manufactured. The prepared ZnO<La> and SnO_2<Co> targets had sufficient conductance and were used for deposition of nanosized films. Multi-Sensor-Platforms (purchased from TESLA BLATNÁ, Czech Republic) are used as substrates. The platform integrates a temperature sensor (Pt 1000), a heater and interdigitated electrode structures with platinum thin film on a ceramic substrate. Heater and the temperature sensor are covered with an insulating glass layer.

Gas sensitive layer made from ZnO doped with 1 at.% La or SnO_2 doped with 2 at.% Co was deposited onto the non-passivated electrode structures using the high-frequency magnetron sputtering method.

The measurements of the manufactured sensors response (the sensor resistance changes under the concentrations of H_2O_2 vapors. The sensor work body temperature was varied from room temperature up to 350 °C. All measurements were carried out at the sensor applied voltage of 0.5 V. The thicknesses of the ZnO doped with 1 at.% La and SnO_2 doped with 2 at.% Co films were equal to 30 nm and 160 nm, respectively. The average size of nanoparticles was equal to 18.7 nm for both compositions. The sensors manufactured by us are resistive. The operation of this type of sensors grounds on the changes in the electrical resistance of gas sensitive semiconductor layer under the influence of H_2O_2 vapors due to an exchange of charges between molecules of the semiconductor film and adsorbed H_2O_2 vapors.

The gas sensing properties of the prepared resistive type gas sensors made from doped metal oxide films under the influence of VPHP were investigated using a computer-controlled static gas sensor home-made test system (see [77]). The sensor was placed in a hermetic chamber. A certain quantity of the H_2O_2 water solution (10 mg) was injected in the measurement chamber. Different concentrations of HPV (from 100 ppm up to 4000 ppm) were reached in the chamber depending on the percentage content of the H_2O_2 water solution.

The measurements of the manufactured sensors' electrical resistance under the VPHP influence were carried out at different operating temperatures. The platinum heater located around the active surface of the sensor on Multi-Sensor-Platform ensures a necessary temperature of the working body. The sensor on alumina substrate is placed on the heater which allows to rise temperature of the sensor's working body. All measurements of the electrical resistance were carried out at 0.5 V DC voltage applied on sensor's electrode.

The typical response-recovery curves obtained in result of these measurements for sensors with $Zn_{0.9929}La_{0.0071}O$ sensitive layer are presented in Fig. 4. These films were deposited on alumina substrate during 15 minutes (Fig. 4(a)) and 30 minutes (Fig. 4(b)) and their thicknesses were equal to 80 nm and 210 nm, respectively. These characteristics demonstrate the change in the sensor's electrical resistance under the influence of 1800 ppm VPHP at different operating temperature.

As a result of the measurements of sensing charcteristics, the sensor response was calculated as the ratio R_{HPV}/R_{air}, where R_{HPV} is the sensor electrical resistance in the VPHP atmosphere and R_{air} is the sensor resistance in the air without VPHP. The results of such calculations of response for the SnO_2<Co> sensor are presented in Fig. 5. These measurements were carried out under the influence of 100 ppm VPHP at different working body temperatures.

The results of investigations of the dependence of the sensor response on operating temperature for sensors with the La-doped ZnO gas sensitive layer are presented in Fig. 6. The concentration of target gas was 1800 ppm in these measurements. At relatively low operating temperature (150 °C), the best response was observed for the structure with larger contents of impurity ($Zn_{0.9853}La_{0.0147}O$). At higher temperatures, sensor with more thick film shows larger response.

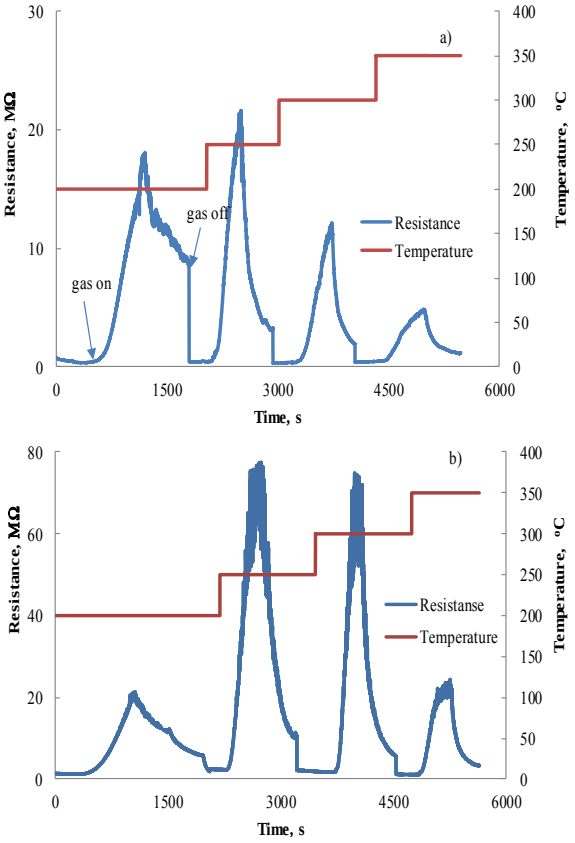

Fig. 4. Response-recovery curves observed under the influence of 1800 ppm VPHP (42-45 % RH) measured at different operating temperatures for the $Zn_{0.9929}La_{0.0071}O$ sensors with films thicknesses of 80 nm (a) and 210 nm (b).

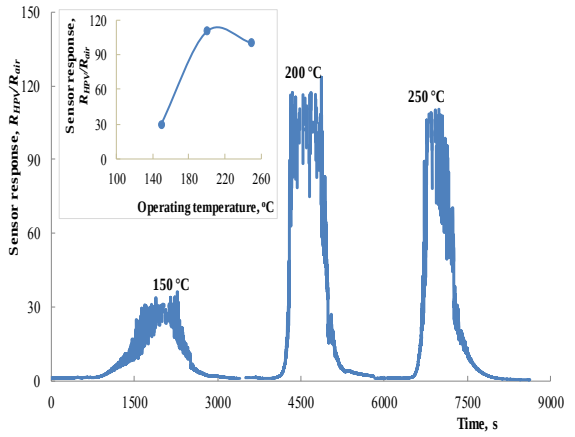

Fig. 5. Response-recovery curves observed under the influence of 100 ppm HPV (42-45 % RH) measured at different operating temperatures for the SnO_2<Co> sensor. Dependence of the sensor response on operating temperature (in insert).

Probably a longer sputtering time allows obtaining a thicker film with more perfect structure. Besides the roughness of the films' surfaces is the same since these sensitive layers were made under identical conditions. However, the working volume and, accordingly, the number of H_2O_2 molecules participating in the charge exchange process are larger for a thicker film.

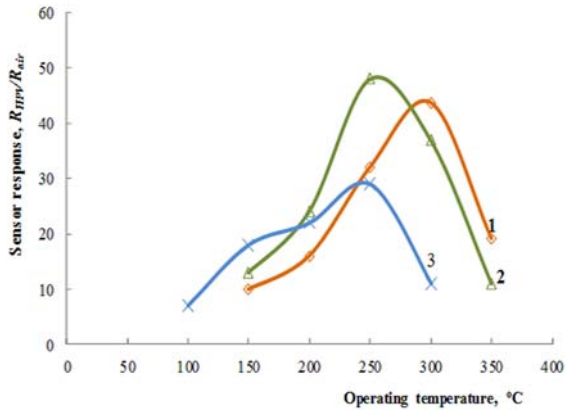

Fig. 6. Dependence of the response to 1800 ppm of VPHP on operating temperature for the $Zn_{0.9929}La_{0.0071}O$ sensors on alumina substrate with films thicknesses of 80 nm (1) and 210 nm (2) and for the sensor with $Zn_{0.9853}La_{0.0147}O$ films deposited on Multi-Sensor-Platform (3).

Note, the electrical resistance of the prepared ZnO<La> sensors has changed in order of magnitude under influence of VPHP starting at operating temperature of 100 °C. However, a longer time needed for recovery of the sensors parameters at such temperature. The pulsed rise in the working body temperature needed for decreasing of the recovery time of the investigated sensors. The response and recovery times were determined when the time required for reaching the 90 % resistance changes from the corresponding steady-state value of each signal. For SnO_2<Co> structure both the response and recovery times were equal to 5 minutes at the temperatures more than 200 °C. For the ZnO<La> sensors the response and recovery times were an average equal to 6-8 minutes and 10-12 minutes, respectively, at the operating temperatures more than 200 °C. The real response times may be less than the mentioned values. This is due to the fact that, as was already noted, 10 mg of an aqueous solution with a certain percentage content of H_2O_2 is injected in measuring chamber in order to obtain the appropriate concentration of VPHP. The response time of the sensor, calculated from the moment when the H_2O_2 water solution is injected in the chamber until the maximum response reaches 90 %, also includes the time necessary for the complete evaporation of the aqueous solution.

As shown in Fig. 5 and Fig. 6, the sensor response decreases for both structures, when the temperature of working body exceeds some certain value (250-300 °C and 200 °C for La-doped ZnO and Co-doped SnO_2 sensors, respectively). The amount of vapor molecules adsorbed on a surface and generally kept by Van der Waals forces (physical adsorption), decreases with the increasing of temperature. More intensive exchange of electrons between the absorber and the absorbed molecules takes place when the stronger chemical nature bond is established between them, originated at capping of electronic shells of both adsorbent and adsorbate atoms. The amount of chemisorbed centers increases with increasing of temperature. Desorption

prevails over the adsorption when a temperature is increased above certain value and, therefore, the sensor response decreases. The temperature of the sensors made of ZnO<La> structure, above which the sensitivity decreasing occurs, is greater than for the sensors made of SnO_2<Co> structure. Probably, the chemical bonds between molecules of ZnO and H_2O_2 are stronger than that between molecules of SnO_2 and H_2O_2. The fact that the recovery time for sensors made of Co-doped SnO_2 is less than that for La-doped ZnO sensors also testifies above-mentioned.

As it has already been noticed, the H_2O_2 belongs to the type of materials dangerous for man after certain maximum permissible concentration. The permissible limit of exposure of 1,0 ppm has established by Occupational Safety and Health Administration (OSHA, USA) [22, 25]. It is immediately dangerous for life and health when its concentration reaches 75 ppm. Therefore, it was necessary to investigate the gas sensing characteristics of prepared sensors made the sensing properties of the prepared sensors with La-doped ZnO and Co-doped SnO_2 sensitive films deposited on Multi-Sensor-Platforms were carried out at less than 100 ppm concentrations of VPHP. The results of these investigations are presented in Fig. 7 and Fig. 8.

The measurements of the sensing characteristics of the sensors with $Zn_{0.9929}La_{0.0071}O$ sensitive layer to 10 ppm VPHP were carried out in the following way. Firstly, an atmosphere containing 10 ppm of VPHP was prepared in a laboratory model of an isolator. This VPHP concentration decreased by spontaneous decomposition of H_2O_2. When a reference device (Dräger Sensor® H_2O_2 HC) could not detect any VPHP, the ZnO<La> sensor was inserted into the model isolator.

Then, the sensor responded immediately. When the maximum response was reached, the sensor was taken out into an atmosphere without any traces of VPHP. This process was repeated three times (Fig. 7(a)). In these studies, a voltage on sensor at direct current is used as a parameter for sensing characteristics. The measurements of the sensing characteristics under the influence of 75 ppm VPHP were carried out using the same way for the SnO_2<Co> sensors (Fig. 7(b)).

The temperature dependence of sensing parameter (or voltage on sensor) under the influence of 10 ppm VPHP was investigated for the SnO_2<Co> sensors. For these measurements the atmosphere in the "Peroxybox" system developed in the same Institute in Prague was controlled (0-10 ppm VPHP and 20-23 % RH) and the sensor's temperature was changed. The final sensitivity was calculated as the voltage on sensor in "Peroxybox" system VPHP divided by voltage on sensor in the air V_{air} (Fig. 8(a)). The temperature dependence of sensing parameter under the influence of 100 ppm VPHP was investigated using the same way for the ZnO<La> sensors (Fig. 8(b)).

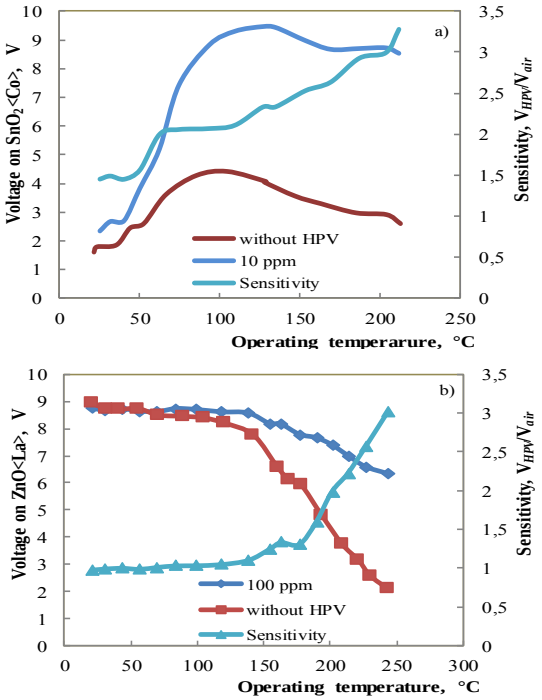

Fig. 7. a) Response-recovery curves observed under the influence of 10 ppm VPHP measured at 220 °C operating temperatures for the $Zn_{0.9929}La_{0.0071}O$ sensor and Dräger Sensor; b) Response-recovery curves observed under the influence of 75 ppm VPHP measured at 200 °C operating temperatures for the SnO_2<Co> sensor.

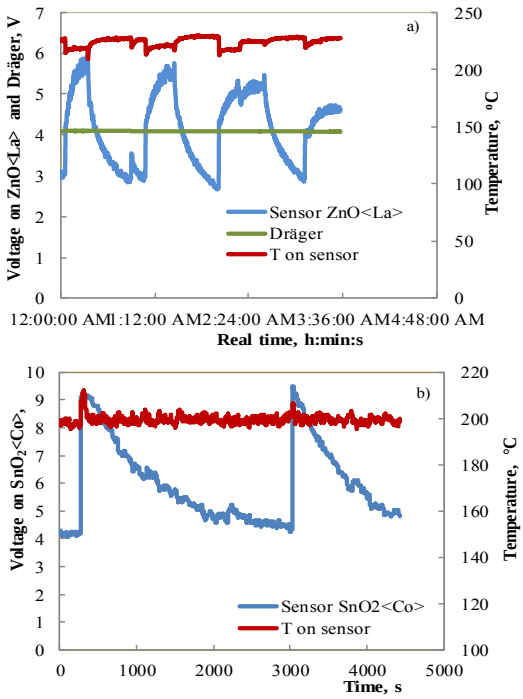

Fig. 8. a) The temperature dependencies of voltage on sensor and sensitivity (V_{HPV}/V_{air}) for SnO_2<Co> sensor measured under the influence of 10 ppm VPHP (20-23 % RH) at 200°C operating temperature; b) The temperature dependencies of voltage on sensor and sensitivity (V_{HPV}/V_{air}) for $Zn_{0.9929}La_{0.0071}O$ sensor measured under the influence of 100 ppm VPHP at 220°C operating temperature.

The investigations of the prepared sensors under the influence of low concentrations of VPHP showed that the sensitivity (V_{HPV}/V_{air}) to 10 ppm of H VPHP was equal to ~ 2 for the ZnO<La> sensors at the working body temperature of 220°C. Note that the DrägerSensor® H_2O_2 HC reference device was not sensitive to 10 ppm of VPHP (Fig. 7(a)). The investigations of the sensors sensitivity to very low concentrations (0-10 ppm) of VPHP showed that the structure made of SnO_2<Co> exhibits a response to 10 ppm of VPHP at the operating temperature starting from 50 °C (Fig. 8(a)). The sensitivity to 10 ppm of VPHP was equal to ~ 3 for the SnO_2<Co> sensors at the working body temperature of 200 °C.

Fig. 9 presents the results of the investigations of the response at the different concentrations of VPHP for the prepared sensors.

As can be seen in Fig. 9, the dependencies of sensor response on VPHP concentration have a linear character for all sensors. Due to the linear dependence of the response on concentration of target gas, it is possible to determinate of VPHP concentration in the environment.

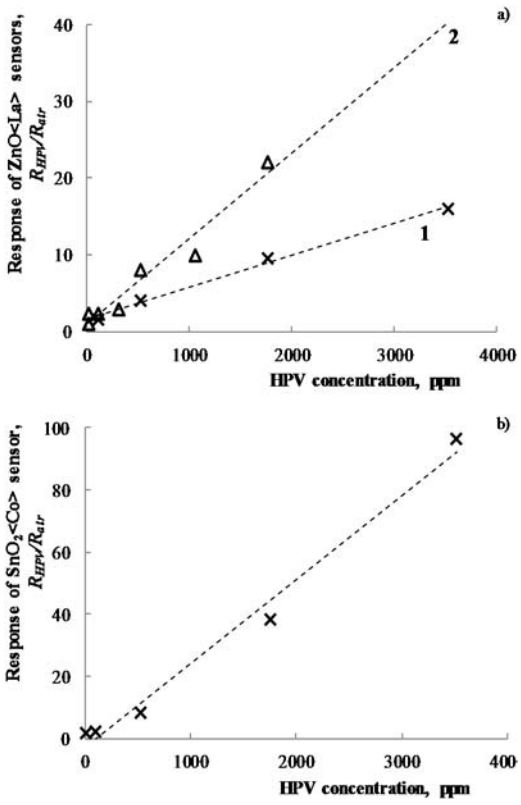

Fig. 9. Dependencies of the response on VPHP concentration measured at 150 °C operating temperature for $Zn_{0.9929}La_{0.0071}O$ (a1), $Zn_{0.9853}La_{0.0147}O$ (a2) and $Sn_{0.9877}Co_{0.0123}O_2$ (b) sensors.

So, it was found that both Co-doped SnO_2 and La-doped ZnO sensors exhibit a good response to VPHP starting at 100°C operating temperature. Sensors made from SnO_2<Co> and ZnO<La> were sufficiently sensitive to 10 ppm of VPHP. It was established that the dependencies of the response on VPHP concentration at the operating temperature of 150°C have a linear character for prepared structures and can be used for determination of VPHP concentration.

This research work was supported by the Swiss National Science Foundation FNSNF support within the framework of the SCOPES DecoComp project. Author express his deep gratitude to co-authors.

6. Conclusion

The H_2O_2 stable sensors can be used in in various fields of the industry and analytical chemistry, for the environmental control, in clinical diagnostic. A large range of materials such as ferric hexacyanoferrate (Prussian blue), metal hexacyanoferrates, etallophthalocyanines and metalloporphyrins, transition metals have been employed earlier. It is necessary now to involve new materials for the manufacture of small size sensors. Recently, linear response to hydrogen peroxide concentration range, high sensitivity, and low detection limit were reported for sensor made from copper and gold nanoparticles dispersed onto polypyrrole (PPy) nanowires. Hydrogen peroxide sensors made from metaloxides TiO_2, n-type CuO nanoparticles (NPs) with p-type semiconductive MnAl layered double hydroxide nanospheres and channels, hollow-sphere Co_3O_4 nanoparticles were reported. A new electrocatalyst, MnO_2/graphene oxide hybrid nanostructure, NiO/graphene and reduced graphene oxide / zinc oxide nanocomposites, reduced graphene oxide co-modified TiO_2 nanotube arrays, $FeVO_4$ nanobelt structures, TiO_2-encapsulated Au yolk-shell nanostructures iron oxide-based nanoparticles with peroxidase, V_2O_5 nanozymes was synthesized and investigated as promising electrodes. Hydrogen peroxide nanosensors for detection of H_2O_2 made from carbon nanotubes were presented. The Ag particles-SWCNT film sensor was investigated.

Vapor phase hydrogen peroxide sensors made from doped metal oxide ZnO<La> and SnO_2<Co> were prepared and investigated in details. It was found that both Co-doped SnO_2 and La-doped ZnO sensors exhibit a good response to VPHP starting at low operating temperature (100°C). Sensors made from SnO_2<Co> and ZnO<La> were sufficiently sensitive to low ppm of VPHP. It was established that the dependencies of the response on VPHP concentration have a linear character for prepared structures and can be used for determination of VPHP concentration.

References

[1]. Y. Tian, F. Wang, Y. Liu, F. Pang, X. Zhang, Green synthesis of silver nanoparticles on nitrogen-doped graphene for H_2O_2 detection, *Electrochim. Acta*, Vol. 146, 2014, pp. 646–653.

[2]. E. W. Miller, S. X. Bian, C. J. Chang, A fluorescent sensor for imaging reversible redox cycles in living

cells, *J. Am. Chem. Soc*., Vol. 129, Issue 12, 2007, pp. 3458–3459.

[3]. F. Ai, H. Chen, S. H. Zhang, S. Y. Liu, F. Wei, X. Y. Dong, J. K. Cheng, W. H. Huang, Real-time monitoring of oxidative burst from single plant protoplasts using micro electrochemical sensors modified by platinum nanoparticles, *Anal. Chem.*, Vol. 81, Issue 20, 2009, pp. 8453–8458.

[4]. Y. Zhang, X. Bai, X. Wang, K. K. Shiu, Y. Zhu, H. Jiang, Highly sensitive graphene-Pt nanocomposites amperometric biosensor and its application in living cell H_2O_2 detection, *Anal. Chem*., Vol. 86, Issue 19, 2014, pp. 9459–9465.

[5]. B. Simen Zhao, Y. Liang, Y. Song, C. Zheng, Z. Hao, P. R. Chen, A highly selective fluorescent probe for visualization of organic hydroperoxides in living cells, *J. Am. Chem. Soc.*, Vol. 132, Issue 48, 2010, pp. 17065–17067.

[6]. H. Zhu, A. Sigdel, S. Zhang, D. Su, Z. Xi, Q. Li, S. Sun, Core/shell Au/MnO_2 nanoparticles prepared through controlled oxidation of AuMn as an electrocatalyst for sensitive H_2O_2 detection, *Angew. Chem. Int. Ed. Engl.*, Vol. 126, 2014, pp. 12508–12512.

[7]. C.-C. Hsu, Y.-R. Lo, Y.-C. Lin, Y.-C. Shi, P.-L. Li, A spectrometric method for hydrogen peroxide concentration measurement with a reusable and cost-efficient sensor, *Sensors,* Vol. 15, Issue 10, 2015, pp. 25716-25729.

[8]. H. A. Rahim, B. C. Morat, R. A. Rahim, Non-invasive evaluation of hydrogen peroxide concentrations in a drinking bottle by near-infrared spectrometry, *Sensors & Transducers*, Vol. 131, Issue 8, August 2011, pp. 83-90.

[9]. J. Sun, C. Li, Y. Qi, S. Guo, X. Liang, Optimizing colorimetric assay based on V_2O_5 nanozymes for sensitive detection of H_2O_2 and glucose, *Sensors*, Vol. 16, Issue 4, 2016, pp. 584-595.

[10]. C.-Y. Lin, C.-T. Chang, Iron oxide nanorods array in electrochemical detection of H_2O_2, *Sensors and Actuators B: Chemical*, Vol. 220, 2015, pp. 695-704.

[11]. A. A. Ensafi, F. Rezaloo, B. Rezaei, Electrochemical sensor based on porous silicon/silver nanocomposite for the determination of hydrogen peroxide, *Sensors and Actuators B: Chemical*, Vol. 231, 2016, pp. 695-704.

[12]. E. A. Puganova, A. A. Karyakin, New materials based on nanostructured Prussian blue for development of hydrogen peroxide sensors, *Sensors and Actuators B: Chemical*, Vol. 109, Issue 1, 2005, pp. 167-170.

[13]. W. Chen, S. Cai, Q.-Q. Ren, W. Wen, Y.-D. Zhao, Recent advances in electrochemical sensing for hydrogen peroxide: a review, *Analyst*, Vol. 137, Issue 1, 2012, pp. 49-58.

[14]. S. Chen, R. Yuan, Y. Chai, F. Hu, Electrochemical sensing of hydrogen peroxide using metal nanoparticles: a review, *Microchimica Acta*, Vol. 180, 2013, pp. 15-32.

[15]. X. Chen, G. Wu, Z. Cai, M. Oyama, Xi Chen, Advances in enzyme-free electrochemical sensors for hydrogen peroxide, glucose, and uric acid, *Microchimica Acta*, Vol. 181, 2014, pp. 689-705.

[16]. B. Šljukič, C. E. Banks, R. G. Compton, Iron oxide particles are the active sites for hydrogen peroxide sensing at multiwalled carbon nanotube modified electrodes, *Nano Letters*, Vol. 6, Issue 7, 2006, pp. 1556-1558.

[17]. F. Pogacean, C. Socaci, S. Pruneanu, A. R. Biris, M. Coros, L. Magerusan, G. Katona, R. Turcu, G. Botodi, Graphene based nanomaterials as chemical sensors for hydrogen peroxide – A comparison study of their intrinsic peroxidase catalytic behavior, *Sensors and Actuators B: Chemical*, Vol. 213, 2015, pp. 474-483.

[18]. X. Yang, Y. Ouyang, F. Wu, Y. Hu, Y. Ji, Z. Wu, Size controllable preparation of gold nanoparticles loading on grapheme sheets@cerium oxide nanocomposites modified gold electrode for nonenzymatic hydrogen peroxide detection, *Sensors and Actuators B: Chemical*, Vol. 238, 2017, pp. 40-47.

[19]. Z.-L. Wu, C.-K. Li, J.-G. Yu, X.-Q. Chen, MnO_2/reduced graphene oxide nanoribbons: facile hydrothermal preparation and their application in amperometric detection of hydrogen peroxide, *Sensors and Actuators B: Chemical*, Vol. 239, 2017, pp. 544-552.

[20]. P. Kačer, J. Švrček, K. Syslová, J. Václavík, D. Pavlík, J. Červený, M. Kuzma, Vapor phase hydrogen peroxide – method for decontamination of surfaces and working areas from organic pollutants, in: Organic pollutants ten years after the Stockholm Convention – environmental and analytical update, *InTech,* Chapter 17, 2012, pp. 399-430.

[21]. I. Taizo, A. Sinichi, K. Kawamura, Application of a newly developed hydrogen peroxide vapor phase sensor to HPV sterilizer, *PDA Journal of Pharmaceutical Science and Technology*, Vol. 52, Issue 1, 1998, pp. 13-18.

[22]. J. Oberländer, P. Kirchner, H.-G. Boyen, M. J. Schöning, Detection of hydrogen peroxide vapor by use of mandanese (IV) oxide as catalyst for calorimetric gas sensors, *Physica Status Solidi A*, Vol. 211, Issue 6, 2014, pp. 1372-1376.

[23]. F. I. Bohrer, C. N. Colesniuc, J. Park, I. K. Schuller, A. C. Kummel, W. C. Trogler, Selective detection of vapor phase hydrogen peroxide with phthalocyanine chemiresistors, *Journal of the American Chemical Society*, Vol. 130, Issue 12, 2008, pp. 3712-3713.

[24]. A. Mills, P. Grosshans, E. Snadden, Hydrogen peroxide vapour indicator, *Sensors and Actuators B: Chemical*, Vol. 136, 2009, pp. 458-463.

[25]. S. Corveleyn, G. M. R. Vandenbossche, J. P. Remon, Near-infrared (NIR) monitoring of H_2O_2 vapor concentration during vapor hydrogen peroxide (VHP) sterilization, *Pharmaceutical Research*, Vol. 14, Issue 3, 1997, pp. 294-298.

[26]. J. Benedet, D. Lu, K. Cizek, J. La Belle, J. Wang, Amperometric sensing of hydrogen peroxide vapor for security screening, *Analytical and Bioanalytical Chemistry*, Vol. 395, Issue 2, 2009, pp. 371-376.

[27]. J. Y. Zheng, Y. Yan, X. Wang, W. Shi, H. Ma, Y. S. Zhao, J. Yao, Hydrogen peroxide vapor sensing with organic core/sheath nanowire optical waveguides, *Sensors & Transducers*, Vol. 213, Issue 6, June 2017, pp. 46-53.

[28]. Martin Novák, Development of Sensor for On-line Monitoring of VPHP Process, Bach. Thesis, *University of Chemistry and Technology*, Prague, 2013, p. 47.

[29]. Tingting Zhang, Ruo Yuan, Yaqin Chai, Wenjuan Li, Shujuan Ling, A novel nonenzymatic hydrogen peroxide sensor based on a polypyrrole nanowire-copper nanocomposite modified gold electrode, *Sensors*, Vol. 8, Issue 8, 2008, pp. 5141-5152.

[30]. Cheng-Chih Hsu, Yuan-Rong Lo, Yu-Chian Lin, Yi-Cen Shi, Pang-Lung Li, A spectrometric method for hydrogen peroxide concentration measurement with a

reusable and cost-efficient sensor, *Sensors*, Vol. 15, 2015, pp. 25716-25729.

[31]. Y. Usui, K. Sato, M. Tanaka, Catalytic dihydroxylation of olefins with hydrogen peroxide: an organic-solvent-and metal-free system, *Angew. Chem.*, Vol. 42, 2003, pp. 5623-5625.

[32]. Soundappan Thiagarajan, Buo-Wei Su, Shen-Ming Chen, Nano Ti_{O2}–Au–KI film sensor for the electrocatalytic oxidation of hydrogen peroxide, *Sensors and Actuators B: Chemical,* Vol. 136, Issue 2, pp. 464-471.

[33]. Muhammad Asifa, Wang Haitaoa, Dong Shuanga, Ayesha Aziza, Guoan Zhanga, Fei Xiao, Hongfang Liu, Metal oxide intercalated layered double hydroxide nanosphere, *Sensors and Actuators B: Chemical,* Vol. 239, 2017, pp. 243-252.

[34]. Mei Wang, Xiaodan Jiang, Junjuan Liu, Hailing Guoa, Chenguang Liu, Highly sensitive H_2O_2 sensor based on Co_3O_4 hollow sphere prepared via a template-free method, *Electrochimica Acta*, Vol. 182, 2015, pp. 613-620.

[35]. W. Chen, S. Cai, Q.-Q. Ren, W. Wen, Y.-D. Zhao, Recent advances in electrochemical sensing for hydrogen peroxide: a review, *Analyst*, Vol. 137, Issue 1, 2012, pp. 49-58.

[36]. W. Jia, M. Guo, Z. Zheng, T. Yu, E. G. Rodriguez, Y. Wang, Y. Lei, Electrocatalytic oxidation and reduction of H_2O_2 on vertically aligned Co_3O_4 nanowalls electrode: toward H_2O_2 detection, *J. Electroanal. Chem.*, Vol. 625, 2009, pp. 27-32.

[37]. C. Hou, Q. Xu, L. Yin, X. Hu, Metal–organic framework templated synthesis of Co_3O_4 nanoparticles for direct glucose and H_2O_2 detection, *Analyst*, Vol. 137, 2012, pp. 5803-5808.

[38]. A. A. Ensafi, M. Jafari–Asl, B. Rezaei, A novel enzyme-free amperometric sensor for hydrogen peroxide based on Nafion/exfoliated graphene oxide-Co_3O_4 nanocomposite, *Talanta*, Vol. 103, 2013, pp. 322-329.

[39]. H. Heli, J. Pishahang, Cobalt oxide nanoparticles anchored to multiwalled carbon nanotubes: Synthesis and application for enhanced electrocatalytic reaction and highly sensitive nonenzymatic detection of hydrogen peroxide, *Electrochim. Acta*, Vol. 123, 2014, pp. 518-526.

[40]. J. Mu, L. Zhang, M. Zhao, Y. Wang, Co_3O_4 nanoparticles as an efficient catalase mimic: Properties, mechanism and its electrocatalytic sensing application for hydrogen peroxide, *J. Mol. Catal. A: Chem.*, Vol. 378, 2013, pp. 30-37.

[41]. S. Xia, M. Yu, J. Hu, J. Feng, J. Chen, M. Shi, X. Weng, A model of interface-related enhancement based on the contrast between Co_3O_4 sphere and cube for electrochemical detection of hydrogen peroxide, *Electrochem. Commun.*, Vol. 40, 2014, pp. 67-70.

[42]. Guiye Shan, Shujing Zheng, Shaopeng Chen, Yanwei Chen, Yichun Liu, Detection of label-free H_2O_2 based on sensitive Au nanorods as sensor, *Colloids and Surfaces B: Biointerfaces*, Vol. 102, 2013, pp. 327-330.

[43]. Limiao Li, Zhifeng Du, Shuang Liu, Quanyi Hao, Yanguo Wang, Qiuhong Li, Taihong Wang, A novel nonenzymatic hydrogen peroxide sensor based on MnO_2/graphene oxide Nanocomposite, *Talanta*, Vol. 82, Issue 5, 2010, pp. 1637-1641.

[44]. Zhiyuan Yu, Hejun Li, Xinmeng Zhang, Ningkun Liu, Xv Zhang, NiO/graphene nanocomposite for determination of H_2O_2 with a low detection limit, *Talanta,* Vol. 144, 2015, pp.1-5.

[45]. Selvakumar Palanisamya, Shen-Ming Chena, Ramiah Sarawathib, A novel nonenzymatic hydrogen peroxide sensor based on reduced graphene oxide/ZnO composite modified electrode, *Sensors and Actuators B: Chemical,* Vol. 166–167, Issue 1, 2012, pp. 372-377.

[46]. Vladimir Aroutiounian, Graphene- and graphene-oxide-based gas sensors, in: Graphene Science Handbook. Applications and Industrialization, *CRC Press Tailor & Francis Group*, USA, Fl., Boca Raton, Chapter 20, 2016, pp. 299-310.

[47]. Z. Wang, X. Zhou, J. Zhang, F. Boey, H. Zhang, Direct electrochemical reduction of single-layer graphene oxide and subsequent functionalization with glucose oxidase, *J. Phys. Chem. C*, Vol. 113, Issue 32, 2009, pp. 14071-14075.

[48]. V. K. Rana, M. C. Choi, J. Y. Kong, G. Y. Kim, M. J. Kim, S. H. Kim, S. Mishra, R. P. Singh, C. S. Ha, Synthesis and drug-delivery behavior of chitosan-functionalized graphene oxide hybrid nanosheets, *Macromol. Mater. Eng.*, Vol. 296, 2011, pp. 131-140.

[49]. X. Wang, L. Zhi, K. Mullen, Transparent, conductive graphene electrodes for dye-sensitized solar cells, *Nano Lett.*, Vol. 8, Issue 1, 2008, pp. 323-327.

[50]. W. Chen, L. Yan, P. R. Bangal, Preparation of graphene by the rapid and mild thermal reduction of graphene oxide induced by microwaves, *Carbon*, Vol. 48, Issue 4, 2010, pp. 1146-1152.

[51]. S. Stankovicha, D. A. Dikina, R. D. Pine, Synthesis of graphene-based nanosheets via chemical reduction of exfoliated graphene oxide, *Carbon*, Vol. 45, Issue 7, 2007, pp. 1558-1565.

[52]. C. Nethravathi, M. Rajamathi, Chemically modified graphene sheets produced by the solvothermal reduction of colloidal dispersions of graphene oxide, *Carbon*, Vol. 46, Issue 14, 2008, pp. 1994-1998.

[53]. Florina Pogaceana, Crina Socacia, Stela Pruneanua, Alexandru R. Birisa, Maria Corosa, Lidia Magerusana, Gabriel Katonab, Rodica Turcua, Gheorghe Borodi, Graphene based nanomaterials as chemical sensors for hydrogen peroxide – A comparison study of their intrinsic peroxidase catalytic behavior, *Sensors and Actuators B: Chemical,* Vol. 213, 2015, pp. 474-483.

[54]. Zhi-Liang Wua, Cheng-Kun Lia, Jin-Gang Yua, Xiao-Qing Chen, MnO_2/reduced graphene oxide nanoribbons: Facile hydrothermal preparation and their application in amperometric detection of hydrogen peroxide, *Sensors and Actuators B: Chemical,* Vol. 239, 2017, pp. 544-552.

[55]. Shan Huanga, Zhichun Sia, Xuankun Lia, Jinshuo Zoua,b, Youwei Yaoa, Duan Wenga, A novel Au/r-GO/TNTs electrode for H_2O_2., O_2 and nitrite detection, *Sensors and Actuators B: Chemical,* Vol. 234, 2016, pp. 264–272.

[56]. Yanzhen Yu, Peng Ju, Dun Zhang, Xiuxun Han, Xiaofei Yin, Li Zheng, Chengjun, Peroxidase-like activity of $FeVO_4$ nanobelts and its analytical application for optical detection of hydrogen peroxide, Sensors and Actuators *B: Chemical,* Vol. 233, 2016, pp. 162-172.

[57]. Xiange Peng, Gengping Wan, Lihong Wu, Min Zeng, Shiwei Lin, Guizhen Wang, Au@TiO_2 yolk-shell nanostructure and its application for colorimetric detection of H_2O_2 and glucose, *Sensors and Actuators B: Chemical,* Vol. 257, 2018, pp. 166-177.

[58]. Jiaheng Sun, Chunyan Li, Yanfei Qi, Shuanli Guo, Xue Liang, Optimizing Colorimetric Assay Based on V_2O_5 Nanozymes for Sensitive Detection of H_2O_2 and Glucose, *Sensors*, Vol. 16, Issue 4, 2016, pp. 584-595.

[59]. Wei H., Wang E. K., Nanomaterials with enzyme-like characteristics (nanozymes): Next-generation artificial enzymes, *Chem. Soc. Rev*., Vol. 42, 2013, pp. 6060-6093.

[60]. Gao L. Z., Zhuang J., Nie L., Zhang J. B., Zhang Y., Gu N., Wang T. H., Feng J., Yang D., Perrete S., *et al*., Intrinsic peroxidase-like activity of ferromagnetic nanoparticles, *Nat. Nanotechnol*, Vol. 2, Issue 9, 2007, pp. 577-583.

[61]. Perez J. M., Iron oxide nanoparticles: Hidden talent, *Nat. Nanotechnology*, Vol. 2, Issue 9, 2007, pp. 535-536.

[62]. Comotti M., Pina C. D., Matarrese R., Rossi M., The Catalytic Activity of "Naked" Gold Particles, *Angew. Chem. Int. Ed*., Vol. 43, 2004, pp. 5812-5815.

[63]. Pirmohamed T., Dowding J. M., Singh S., Wasserman B., Heckert E., Karakoti A. S., King J. E. S., Seal S., Self W. T., Nanoceria exhibit redox state-dependent catalase mimetic activity, *Chem. Commun*., Vol. 46, 2010, pp. 2736-2738.

[64]. Mu J. S., Wang Y., Zhao M., Zhang L., Intrinsic peroxidase-like activity and catalase-like activity of Co_3O_4 nanoparticles, *Chem. Commun*., Vol. 48, 2012, pp. 2540-2542.

[65]. Yin J. F., Cao H. Q., Lu Y. X., Self-assembly into magnetic Co_3O_4 complex nanostructures as peroxidase, *J. Mater. Chem*., Vol. 22, 2012, pp. 527-534.

[66]. Chen W., Chen J., Feng Y. B., Hong L., Chen Q. Y., Wu L. F., Lin X. H., Xia X. H., Peroxidase-like activity of water-soluble cupric oxide nanoparticles and its analytical application for detection of hydrogen peroxide and glucose, *Analyst*, Vol. 137, Issue 7, 2012, pp. 1706-1712.

[67]. Wan Y., Qi P., Zhang D., Wu J. J., Wang Y., Manganese oxide nanowire-mediated enzyme-linked immunosorbent assay, *Biosens. Bioelectron*., Vol. 33, Issue 1, 2012, pp. 69-74.

[68]. André R., Natálio F., Humanes M., Leppin J., Heinze K., Wever R., Schröder H.-C., Müller W. E. G., Tremel W., V_2O_5 Nanowires with an intrinsic peroxidase-like activity, *Adv. Funct. Mater*., Vol. 21, Issue 3, 2011, pp. 501-509.

[69]. Shi W. B., Wang Q. L., Long Y. J., Cheng Z. L., Chen S. H., Zheng H. Z., Huang Y. M., Carbon nanodots as peroxidase mimetics and their applications to glucose detection, *Chem. Commun*., Vol. 47, Issue 23, 2011, pp. 6695-6697.

[70]. Song Y. J., Qu K. G., Zhao C., Ren J. S., Qu X. G., Graphene Oxide: Intrinsic Peroxidase Catalytic Activity and Its Application to Glucose Detection, *Adv. Mater*., Vol. 22, Issue 19, 2010, pp. 2206-2210.

[71]. V. M. Aroutiounian, Gas sensors based on functionalized carbon nanotubes, *Journal of Contemporary Physics (Armenian Academy of Sciences)*, Vol. 50, Issue 4, 2015, pp. 333-354.

[72]. V. M. Aroutiounian, A. Z. Adamyan, E. A. Khachaturyan, Z. N. Adamyan, K. Hernadi, Z. Pallai, Z. Nemeth, L. Forro, A. Magrez, E. Horvath, Study of the surface-ruthenated SnO_2/MWCNTs nanocomposite thick-film gas sensors, *Sensors and Actuators B: Chemical*, Vol. 177, 2013, pp. 308-315.

[73]. Vladimir Aroutiounian, Zaven Adamyan, Artak Sayunts, Emma Khachaturyan, Arsen Adamyan, Klara Hernadi, Zoltan Nemeth, Peter Berki, Comparative Study of VOC Sensors Based on Ruthenated MWCNT/SnO_2 Nanocomposites, *Int. J. of Emerging Trends in Science and Technology (IJETST)*, Vol. 01, Issue 08, 2014, pp. 1309-1319.

[74]. V. M. Aroutiounian, Metal oxide gas sensors decorated with carbon nanotubes, *Lithuanian Journal of Physics*, Vol. 55, Issue 4, 2015, pp. 319-329.

[75]. Vladimir M. Aroutiounian, Zaven N. Adamyan, Artak G. Sayunts, Emma A. Khachaturyan, Arsen Z. Adamyan, Study of MWCNT/SnO_2 Nanocomposite acetone and toluene vapor sensors, in *Proceedings of the 17 Int. Conference on Sensors and Measurement Technology (SENSOR 2015)*, Nierenberg, Germany, 19-21 May 2015, pp. 836-841.

[76]. Zaven Adamyan, Artak Sayunts, Vladimir Aroutiounian, Emma Khachaturyan, Arsen Adamyan, Martin Vrnata, Přemysl Fitl, Jan Vlček, Study of Propylene Glycol, Dimethylformamide and Formaldehyde Vapors Sensors Based on MWCNTs/SnO_2 Nanocomposites, *Sensors & Transducers*, Vol. 213, Issue 6, June 2017, pp. 38-45.

[77]. Adamyan Z., Sayunts A., Aroutiounian V., Khachaturyan E., Vrnata M., Fitl P., Vlček J., Nanocomposite sensors of propylene glycol, dimethylformamide and formaldehyde vapors, *J. Sens. Sens. Syst.*, Vol. 7, 2018, pp. 31-41.

[78]. Jing Li, Yijiang Lu, Hydrogen Peroxide Detection Using Carbon Nanotube Sensors, in *Proceedings of the 211th ECS Meeting*, Abstract #1353, The Electrochemical Society, 2006.

[79]. Minh-Phuong Ngoc Bui, Xuan-Hung Pham, Kwi Nam Han, Cheng Ai Lia, Yong Shin Kimb, Gi Hun Seong, Electrocatalytic reduction of hydrogen peroxide by silver particles patterned on single-walled carbon nanotubes, *Sensors and Actuators B: Chemical,* Vol. 150, Issue 1, 2010, pp. 436-441.

[80]. Vladimir Aroutiounian, Valeri Arakelyan, Mikayel Aleksanyan, Artak Sayunts, Gohar Shahnazaryan, Petr Kačer, Pavel Picha, Jiri Kovarik, Jakub Pekarek, Berndt Joost, Nanostructured Sensors for Detection of Hydrogen Peroxide Vapors, *Sensors & Transducers*, Vol. 213, Issue 6, June 2017, pp. 46-53.
